Neutrondiffraction study of cubic ErC0.6 in the temperature range 1.6–296 K

Masao Atoji

Citation: J. Chem. Phys. **74**, 1898 (1981); doi: 10.1063/1.441281
View online: http://dx.doi.org/10.1063/1.441281
View Table of Contents: http://jcp.aip.org/resource/1/JCPSA6/v74/i3
Published by the American Institute of Physics.

Neutron-diffraction study of cubic $ErC_{0.6}$ in the temperature range 1.6–296 K[a)]

Masao Atoji

Chemistry Division, Argonne National Laboratory, Argonne, Illinois 60439
(Received 13 August 1980; accepted 13 October 1980)

Neutron-diffraction measurements have shown that the form of $ErC_{0.6}$ that has a cubic, NaCl-type structure is paramagnetic above 90 K, exhibiting a free Er^{3+} moment. Below 90 K, $ErC_{0.6}$ becomes a ferromagnet with a saturation moment of 2.5 Bohr magnetons (only 28% of the maximum free-ion moment), indicating a large crystal-field effect. By measuring the preferential crystallite orientation induced by the applied magnetic field, the direction of the ferromagnetically ordered moment was found to be parallel to the ⟨100⟩ axis. A ferromagnetic, short-range ordering coexists with the ferromagnetic long-range ordering at temperatures down to 1.6 K.

I. INTRODUCTION

In the phase immediately below the melting point, the rare-earth hypocarbide REC_x (RE = Sm–Lu, Y and $0.25 < x < 0.65$) forms a cubic, NaCl-type structure in which the anion sites are partially occupied by carbon atoms.[1–4] If x is close to 0.5, the structure transforms at lower temperatures (for example, below 1570 K in $YC_{0.5}$) to a trigonal structure, but if x is different from 0.5, the cubic structure is retained at all temperatures.[2–4] We designate the cubic and trigonal structures as REC_x and RE_2C, respectively, so that, for example, $ErC_{0.5}$ is cubic, while Er_2C is trigonal. An inhomogeneous ErC_x in the high-temperature phase may transform to an admixture of the cubic and trigonal structures in the low-temperature phase.[4] For example, an inhomogeneous sample with overall composition $ErC_{0.6}$ may segregate into $0.1\ Er_2C + 0.8\ ErC_{0.63}$. The structural details of the cubic–trigonal transition have been elucidated by Atoji and Kikuchi,[4] using a YC_x single crystal in which the transient state in the midst of the cubic–trigonal transition was arrested.

In a neutron magnetic structure study, Lallement[2] postulated a HoN-type, retarded, ferrimagnetic ordering[5] in Ho_2C at 4 K, on the basis of a broadened-peak appearance. Atoji[6] found that Tb_2C becomes a uniaxial ferromagnet below 266 K, with the ordered moments aligned parallel to the trigonal axis. Hence, Tb_2C is isostructural with Ho_2C in the atomic structure, but not in the magnetic structure.

The magnetic structure of the NaCl-type rare-earth hypocarbide is unknown, and hence the present ErC_x study was undertaken. Lallement[2] has reported some of the physical properties of the cubic form of ErC_x. The paramagnetic susceptibility of an $ErC_{0.45}$ sample containing Er metal impurity gave the effective Bohr magneton number $\mu_{eff} = 8.5$ Bohr magnetons (μ_B), which is somewhat smaller than the 9.58 μ_B of the free Er^{3+} ion. He also observed that $ErC_{0.45}$ becomes ferromagnetic at low temperature. However, the detailed magnetic susceptibility data were not presented. The electrical resistivity and the thermoelectric power of $ErC_{0.4}$ samples containing Er metal impurity, in the range of 4–320 K, are analogous to those of Er_2C, and show broad anomalies, implying transition temperatures in the range 60–100 and 20–50 K, respectively. Lallement gave a qualitative interpretation of these physical properties using the RKKY and crystal-field theories.

II. EXPERIMENTAL AND CRYSTAL STRUCTURE

Erbium hypocarbide samples were prepared by arc melting compressed pellets composed of the filings of distilled erbium metal (99.9% pure) and spectroscopic-grade graphite powder. During the arc melting, despite an environment of comparatively high pressure (about 1 atm) of dry argon gas, the evaporation loss was as much as several percent. Also, the vapor-deposited material in the arc furnace is highly pyrophoric in air. Because of these difficulties, many trial arc meltings were needed to attain the required composition and homogeneity. $ErC_{0.6}$ boules are metallic gray and decompose readily in moist air. Chemical analysis indicated that the sample chosen is ErC_x with $x = 0.6(1)$, where the number in parentheses is the estimated standard deviation of the last significant digit. As described later, the neutron-intensity analysis gave a more precise value of $x = 0.60(2)$.

The diffraction data were taken with 1.069 Å neutrons using both hard-packed and loosely packed powder samples. The latter were used to facilitate preferential crystallite orientation in an applied magnetic field. All the coherent reflections at 296 K [see Fig. 1(A)] were interpreted satisfactorily based on the NaCl-type cubic structure (space group O_h^5-$Fm3m$) with $a = 5.0214(4)$ Å, in agreement with previously reported values.[1,2] Ordering in the carbon-site occupation would give rise to various superlattice reflections, but none were detected in the temperature region 1.6–296 K. Also, no reflections attributable to the trigonal form were observed, implying a high homogeneity of the sample.

The structure refinement, using a weighted least-squares method, led to the temperature factor coefficient $2B = 1.48(8)$ Å^{-2} and $x = 0.60(2)$. The latter signified that the intensities are highly sensitive to the carbon content. The nuclear-scattering lengths used were

[a] Work performed under the auspices of the Office of Basic Energy Sciences, Division of Materials Sciences, U. S. Department of Energy.

 0021-9606/81/031898-04$01.00

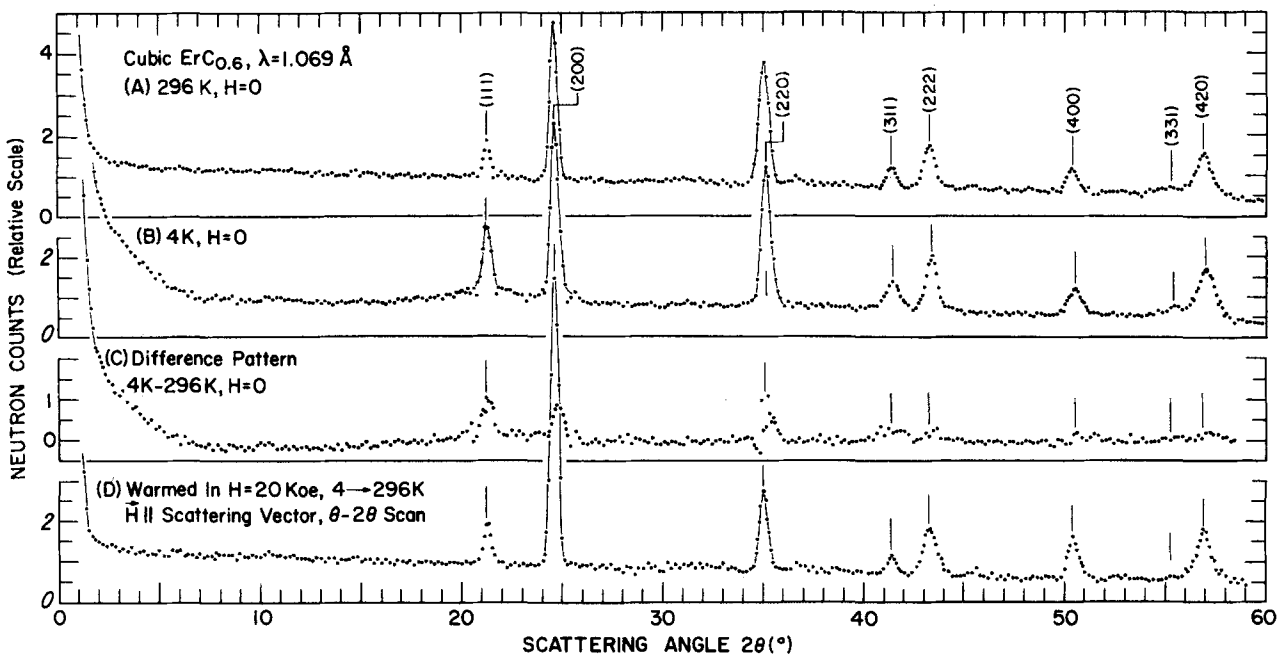

FIG. 1. Neutron-powder diffraction patterns of cubic $ErC_{0.6}$. Patterns (A) and (B) are taken in zero magnetic field at 296 and 4 K, respectively. Pattern (C) is obtained by subtracting (B) from (A) and consists of the magnetic coherent and incoherent scattering. The pattern (D) was obtained by a $\theta-2\theta$ scan of the sample, after it had been warmed from 4 to 296 K in a magnetic field of 21 kOe, applied parallel to the scattering vector. Hence, the coherent peaks in (D) are the nuclear reflections of the preferential crystallite orientation which were induced by the magnetic field in the ferromagnetic phase. The comparison between (A) and (D) indicates that the ordered moment is parallel to the ⟨100⟩.

0.75 and 0.665 (in 10^{-14} m) for Er and C, respectively.[7] The observed and calculated structure factors are listed in Table I. The agreement factor $R=\sum||F_{obs.}|-|F_{calc.}||/\sum|F_{obs.}|$ is 1.5%. The agreement did not improve appreciably by introducing anisotropic or individual temperature factors.

The coherent reflections at 4 K [Fig. 1(B)] and those in the regional scans at 1.6 K indicated that the atomic structure is virtually unchanged in the range of 1.6–296 K. The lattice parameter is $a=5.0108(6)$ Å at 4 K. Hence, the average linear thermal-expansion coefficient over this range is $7.2(5)\times10^{-6}$ deg^{-1}, which is typical of most metallic compounds, and thus indicates no anomalously large magnetostriction below 296 K.

III. MAGNETIC STRUCTURE

The coherent reflections at 4 K [Fig. 1(B)] possess small excess intensities which are satisfactorily accounted for by assigning a ferromagnetically ordered moment of $gJ=2.5(1)\ \mu_B$ per Er atom. The observed and calculated values for the nuclear and magnetic intensities at 4 K are listed in Table II, where the temperature-factor coefficient used is $2B=0.7(1)$ Å^{-2} and the agreement factor $R=\sum|I_{obs.}-I_{calc.}|/\sum I_{obs.}$ is 0.7%.

The direction of the ferromagnetic moment in crystals with cubic symmetry cannot be determined directly by the powder-diffraction method,[8] but it can be determined by inducing a preferential crystallite orientation with an applied magnetic field.[9] The net moment of the crystallite tends to align in the direction of the applied field. The resultant preferential orientation axis can be determined by a $\theta-2\theta$ scan, with the magnetic field applied parallel to the scattering vector. However, the effect of the preferred orientation on the nuclear intensity is quite different from that on the magnetic intensity. Hence, the preferred orientation was induced in

TABLE I. Observed and calculated structure factors in 10^{-14} m per $ErC_{0.6}$ at 296 K.

Indices	$F_{obs.}$	$F_{calc.}$
111	0.388	0.383
200	1.140	1.155
220	1.134	1.121
311	0.347	0.361
222	1.085	1.089
400	1.089	1.057
331	0.351	0.340
420	1.022	1.027

TABLE II. Observed and calculated intensities in 10^{-28} m^2 per $ErC_{0.6}$ at 4 K.

Indices	I_{obs}	I_{calc} (nuclear)	I_{calc} (magnetic)	I_{calc} (total)
111	48	18	29	47
200	108	93	15	108
220	104	92	12	104
311	31	15	14	29
222	45	41	4	45
400	25	23	2	25
331	13	8	5	13
420	79	74	5	79

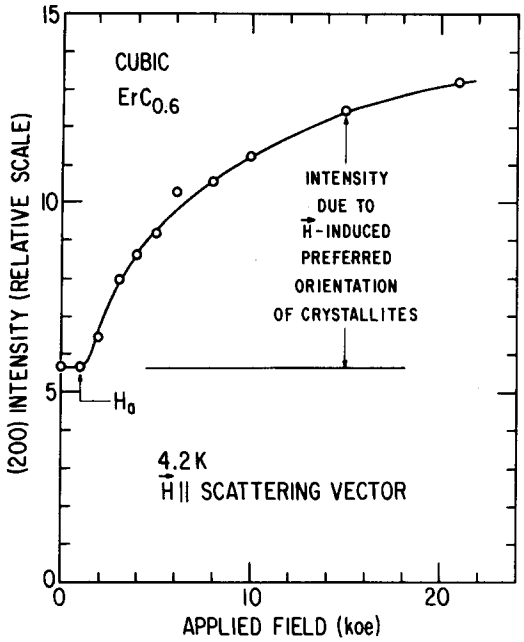

FIG. 2. The intensity of the (200) reflections at 4.2 K as a function of the magnetic field that is applied parallel to the scattering vector. The intensity at $H=0$ consists of about 86% nuclear intensity and 14% magnetic intensity. The magnetic field of about 1 kOe (H_a) is needed to overcome the steric hindrance in the powder packing and to start the orientation of the crystallites. When H increases beyond H_a, the intensity increases due to the nuclear intensity of the preferential crystallite orientation.

the ferromagnetic phase, but the intensity data were collected in the paramagnetic phase, in order to eliminate the magnetic intensity.

In practice, the preferred orientation effect was first examined, as a function of the applied field, at 4 K in order to ensure suitable intensity modulation (Fig. 2). The preferentially oriented crystallites were then warmed up carefully above T_c, without disturbing the powder packing. Because often unavoidable vibrational disturbances can alter the powder packing during experimental procedures, the applied magnetic field was kept on during the warming period. The diffraction pattern thus obtained is shown in Fig. 1(D). It is obvious that the preferential axes, and hence the moment directions, are the ⟨100⟩ axes. Diffraction intensities for preferred orientation in cubic powders have been formulated by Järvinen *et al.*[10]

The magnetic reflection superimposes on the nuclear reflection and is comparatively weak. As a result, the temperature dependency of the magnetic intensity was difficult to measure, particularly near the Curie temperature. The polarized-neutron technique[8] can separate the magnetic intensity from the nuclear intensity, but it was not readily available. Hence the field-induced preferred orientation technique was employed for determing the Curie temperature. The experimental result obtained is $T_c=90(2)$ K, as shown in Fig. 3.

Paramagnetic scattering was obtained by subtracting attenuation-corrected, instrumental scattering (including the incident beam) and incoherent scattering (thermal, nuclear, and multiple) from the total background.[11] The paramagnetic diffuse scattering at 296 K gave the effective Bohr magneton number $\mu_{eff}=9.4(2)\ \mu_B$ of the free Er^{3+} ion. A small hump near $\sin\theta=0$ is probably due to a weak ferromagnetic short-range ordering. The humpy modulation of the scattering curve becomes more pronounced at lower temperatures down to 1.6 K. This implies that the ferromagnetic short-range ordering coexists with the ferromagnetic long-range ordering.[12]

The magnetic diffuse scattering at 4 K was analyzed using a first-order approximation of the short-range order formula[13]

$$\frac{d\sigma}{d\omega}=\frac{2}{3}\left(\frac{e^2\gamma}{2mc^2}\right)^2\mu_{eff}^2 f_m^2\left(1-\frac{2\mu_{eff}^2}{3kT}\sum_n J_n z_n\frac{\sin X_n}{X_n}\right),$$

where $d\sigma/d\omega$ is the differential scattering cross section in b/sr/Er^{3+}; the first term represents the paramagnetic scattering, and the second term represents the short-range order effect; γ is the neutron magnetic moment in nuclear Bohr magnetons; f_m is the magnetic form factor; J_n is proportional to the exchange interaction between the given atom and the nth neighboring atom; z_n is the number of the nth neighbors; and $X_n=4\pi r_n\times(\sin\theta)/\lambda$, r_n being the distance to the nth neighbor. The median curve of the observed data was fitted approximately by $\mu_{eff}=9.2(2)\mu_B$, which approximates $[(\mu_{eff}$ for free ion$)^2$-(ordered moment$)^2]^{1/2}=[(9.45^2-2.5^2)]^{1/2}=9.25\ \mu_B$. Although no unique curve fitting was obtained in the short-range order terms, a first-neighbor interaction curve is shown in Fig. 4 for an

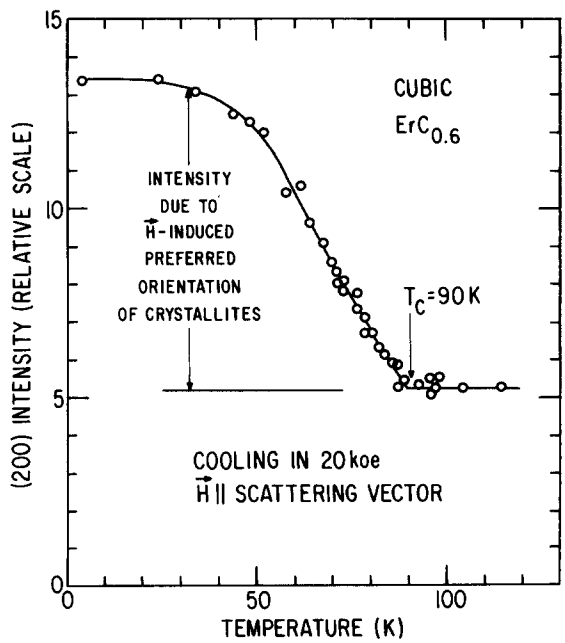

FIG. 3. Determination of the Curie temperature of $ErC_{0.6}$ by the temperature dependence of the (200) intensity in cooling. The 21 kOe field is applied parallel to the scattering vector. The intensity enhancement involves the nuclear contributions only and is proportional to the field-induced preferred orientation of the crystallites and hence to approximately the square of the ferromagnetic moment.

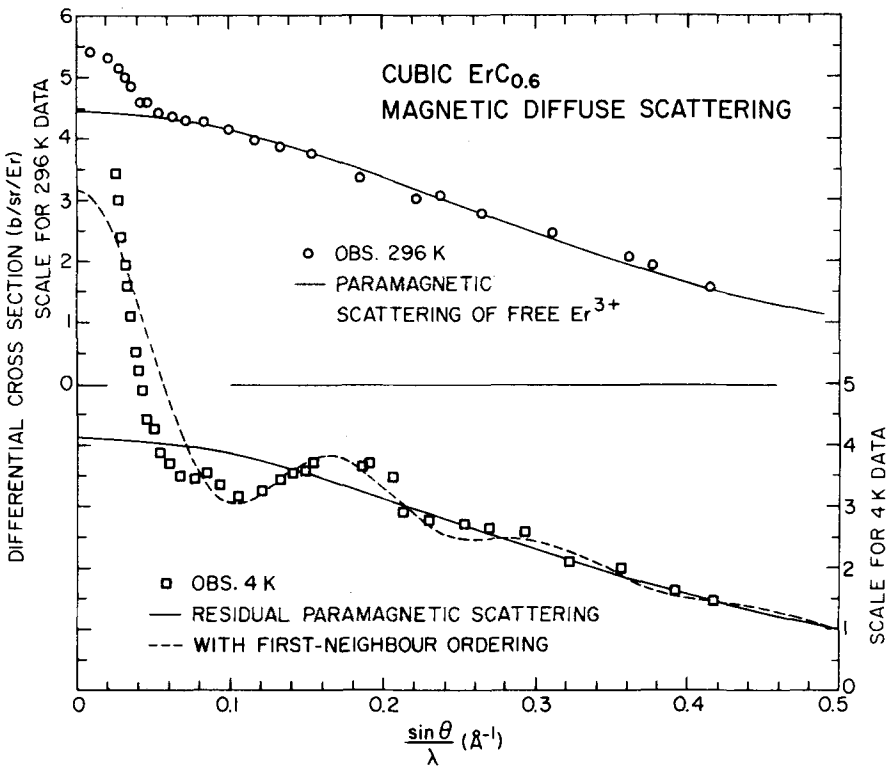

FIG. 4. Observed incoherent magnetic-scattering cross sections of $ErC_{0.6}$ at 297 and 4 K are given in open circles and open squares, respectively. The calculated curves for the incoherent magnetic scattering in the disordered moments and those with the ferromagnetic first-neighbor ordering are given in solid and broken lines, respectively.

example using a ferromagnetic $J_1 = -0.0056k$. A very strong intensity in the vicinity of $\sin\theta = 0$ consists of all the ferromagnetic short-range orderings at the maximum values and an intense, coherent ferromagnetic reflection at $h = k = l = 0$.

IV. DISCUSSION

The physical properties of the NaCl-type rare-earth compounds have been studied rather extensively.[14] In the NaCl-type Er compounds, we compare the pertinent magnetic and related properties (lattice parameter, magnetic transition temperature, ordered moment, respectively), as follows: ErN (4.83 Å, 5 K, 5 μ_B), $ErC_{0.6}$ (5.02 Å, 90 K, 2.5 μ_B), ErP (5.60 Å, 3 K, unknown), ErSb (6.10 Å, 4 K, 7 μ_B), and ErBi (6.19 Å, 4 K, unknown). The Er–Er distance, as inferred from the lattice parameter, is considerably shorter in ErN and $ErC_{0.6}$ than in the others. Correspondingly, the ordered moments are ferromagnetic, and parallel to [100], in ErN and $ErC_{0.6}$, while they are antiferromagnetic, and parallel to [111], in the orders. The variation in the moment direction is due to the different ratios of the crystal-field parameters K_4 and K_6.[12] In all except $ErC_{0.6}$, the ordering temperature is very low, and the ordered moment is suppressed considerably, meaning that the exchange energy is small compared to the overall crystal-field splitting.

$ErC_{0.6}$ exhibits a similarly small ordered moment but a singularly high ordering temperature. This is probably due to the fact that the random carbon distribution results in an assembly of different local crystal fields. For instance, a certain Er atom may have three first-neighbor carbon atoms in an asymmetric configuration, while another Er site may have all 12 first-neighbor carbon atoms. Consequently, the exchange energy between some pairs of Er atoms can be larger than the crystal-field splitting, while a reversed relation may be found between other pairs of Er atoms. Hence, at the former Er sites, the magnetic ordering takes place at relatively high temperature, subsequently inducing a long-range ferromagnetic coupling throughout all Er sites. However, the ordered moments are averaged out to a small value, as observed.

[1] F. H. Spedding, K. Gshneidner, Jr., and A. H. Daane, J. Am. Chem. Soc. 80, 4499 (1958).
[2] R. Lallement, Centre d'Etudes Nucléaires de Fonteney-aux-Roses Rapport, CEA-R 3043, 1966.
[3] G. L. Bacchella, P. Meriel, M. Pinot, and R. Lallement, Bull. Soc. Fr. Mineral. Cristallogr. 89, 226 (1966).
[4] M. Atoji and M. Kikuchi, J. Chem. Phys. 51, 3863 (1960); Argonne National Laboratory Report ANL-7441 (1968).
[5] H. R. Child, M. K. Wilkinson, J. W. Cable, W. C. Koehler, and E. O. Wollan, Phys. Rev. 131, 922 (1963).
[6] M. Atoji, J. Chem. Phys. 51, 3872 (1969).
[7] G. E. Bacon, Acta Crystallogr. Sect. A 28, 357 (1972).
[8] G. E. Bacon, *Neutron Diffraction* (Clarendon, Oxford, 1975), 3rd edition.
[9] M. Atoji, I. Atoji, C. Do-Dinh, and W. E. Wallace, J. Appl. Phys. 44, 5096 (1973).
[10] M. Järvinen, M. Mevisalo, A. Pesonen, and O. Inkinen, J. Appl. Crystallogr. 3, 313 (1970).
[11] M. Atoji, J. Chem. Phys. 35, 1950 (1961); 46, 1891 (1967).
[12] G. T. Trammell, Phys. Rev. 131, 932 (1963).
[13] M. Slotnick, Phys. Rev. 83, 1226 (1951).
[14] F. Hulliger, "Rare Earth Pnictides," in *Handbook on the Physics and Chemistry of Rare Earths*, edited by K. A. Gschneidner, Jr. and LeRoy Eyring (North-Holland, Amsterdam, 1979), Vol. 4, Chap. 33.